Greenberger-Horne-Zeilinger states in a quantum dot molecule

Anand Sharma[*] and Pawel Hawrylak[†]

Department of Physics, University of Ottawa, Ottawa, Canada, K1N6N5 and
Institute for Microstructural Sciences, National Research Council of Canada, Ottawa, Canada, K1A0R6

We present a microscopic theory of a lateral quantum dot molecule in a radial magnetic field with a Greenberger-Horne-Zeilinger (GHZ) maximally entangled three particle ground state. The quantum dot molecule consists of three quantum dots with one electron spin each forming a central equilateral triangle. The antiferromagnetic spin-spin interaction is changed to the ferromagnetic interaction by additional doubly occupied quantum dots, one dot near each side of a triangle. The magnetic field is provided by micromagnets. The interaction among the electrons is described within an extended Hubbard Hamiltonian which is solved by using exact diagonalization techniques. The set of parameters is established for which the ground state of the molecule in a radial magnetic field is well approximated by a GHZ state.

I. INTRODUCTION

In a recent work, Roethlisberger *et al.*[1] proposed a scheme to generate a maximally entangled Greenberger-Horne-Zeilinger[2] (GHZ) state as a ground state of a three spin system. The spins were arranged in a triangular geometry and assumed to interact ferromagnetically. With ferromagnetic interaction the degenerate ground state is maximally spin polarized, with two $|\uparrow\uparrow\uparrow\rangle$ and $|\downarrow\downarrow\downarrow\rangle$ configurations. When the radial in-plane magnetic field is applied the two spin polarized configurations form the two GHZ states $|\text{GHZ}^{\pm}\rangle = \frac{1}{\sqrt{2}}(|\uparrow\uparrow\uparrow\rangle \pm |\downarrow\downarrow\downarrow\rangle)$. Such GHZ ground states of spin molecules could be used as long-lived sources of entanglement.[3,4] One can envisage using lateral triple quantum dot molecules[5–7] with one electron on each dot to realize a three spin system. However, the spin-spin interaction in quantum dot molecules is necessarily antiferromagnetic and such a simple quantum dot molecule is not possible. Here we propose a more complex molecule which uses auxiliary quantum dots to effectively change the spin-spin interaction to ferromagnetic and generate the maximally entangled GHZ state as its ground state.

Theoretical proposals to realize GHZ states in solid state systems include spin systems,[1] excitons in coupled dots,[8] two-level atoms in a nonresonant cavity,[9] and superconducting flux qubits.[10] The GHZ states have been experimentally realized using photons,[11] in atomic systems using three Rydberg atoms,[12] and very recently maximally entangled GHZ states have been realized in a solid state system using superconducting qubits.[13,14] We refer the reader to Refs. 13 and 14 for the full initialization, characterization, and readout of GHZ states.

In this paper, we propose a theoretical model of six coupled quantum dots[6,7,15,16] with interacting electrons to generate the GHZ state as a ground state. The model consists of three equally spaced quantum dots with one electron spin each. The antiferromagnetic interaction of each pair of localized spins is modified by connecting each pair of spins to an auxiliary quantum dot with two electrons. In Ref. 17 it was shown that the effective interaction between two electrons in two quantum dots (i.e., one electron in each of the two quantum dots) can be changed from antiferromagnetic to ferromagnetic

by connecting them to a third (auxiliary) doubly occupied quantum dot and applying a bias to the auxiliary quantum dot. Thus it was shown that there exists a set of parameters for which such a triple quantum dot molecule with four electrons can be thought of as effectively two localized electron spins interacting ferromagnetically. Following this idea, we propose here a quantum dot molecule consisting of three dots with one electron each and three auxiliary dots with two electrons each, which effectively realizes the ferromagnetically coupled three spin cluster. Using the Hubbard model and exact diagonalization techniques we show that the ground state of such a molecule in a radial magnetic field is indeed a GHZ state.

The structure of the paper is organized as follows. In Sec. II we examine the proposed setup for generating highly entangled states in a three spin system interacting ferromagnetically with each other and coupled to a radial in-plane magnetic field. We clarify the role of the applied magnetic field in generating the GHZ states using the degenerate perturbation theory. In Sec. III we propose a quantum dot molecule consisting of six quantum dots with nine electrons and micromagnets to generate the radial in-plane magnetic field creating the maximally entangled GHZ state as its ground state. We describe the system, its Hamiltonian, and ground state phase diagram. The last section, Sec. IV, contains the summary and conclusions.

II. GENERATING GHZ STATE IN A THREE SPIN SYSTEM

We begin with an analysis of the three spin system to create the maximally entangled states as outlined in Ref. 1. The three spins $\frac{1}{2}$ placed at the corners of an equilateral triangle lying in the *xy* plane as shown in the left panel of Fig. 1 are described by an isotropic Heisenberg Hamiltonian,

$$H_{\text{H}} = -J \sum_{i=1}^{3} \mathbf{S}_i \cdot \mathbf{S}_{i+1}, \quad (\mathbf{S}_4 = \mathbf{S}_1), \tag{1}$$

where it is assumed that the exchange coupling J is ferromagnetic ($J > 0$) and $\mathbf{S}_i = \frac{\hbar}{2}(\sigma_i^x, \sigma_i^y, \sigma_i^z)$ is a vector consisting
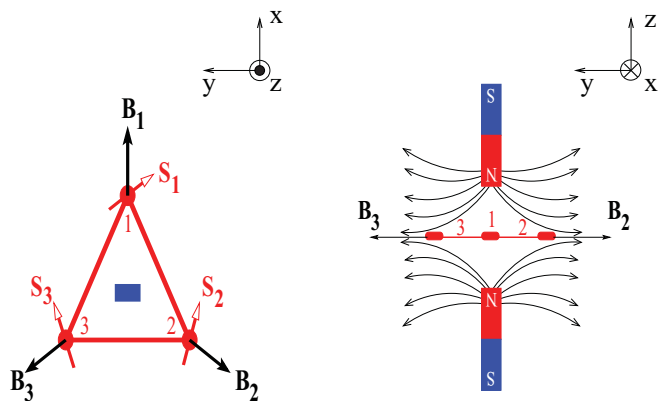
FIG. 1. (Color online) Schematic showing two views of three localized electron spins $S_i (i = 1,2,3)$ arranged in a triangular geometry and interacting ferromagnetically with each other. The two bar magnets at the triangle centroid are placed on top of each other generating a radial magnetic field B_i. Figure on the left shows the top view of such a system and the right panel exhibits the lateral view. The magnetic field lines are also shown.

of Pauli matrices, $\sigma_i^x = \begin{pmatrix} 0 & 1 \\ 1 & 0 \end{pmatrix}$, $\sigma_i^y = \begin{pmatrix} 0 & -i \\ i & 0 \end{pmatrix}$, and $\sigma_i^z = \begin{pmatrix} 1 & 0 \\ 0 & -1 \end{pmatrix}$ acting on sites i (=1,2,3). Here $\hbar$ is a reduced Planck constant.

We write the Hamiltonian, given in Eq. (1), in the basis of the tensor product of states at each site. For example, the Pauli matrices are written in such a local basis. Thus the Hamiltonian in the basis set $\{|\uparrow\uparrow\uparrow\rangle, |\uparrow\uparrow\downarrow\rangle, |\uparrow\downarrow\uparrow\rangle, |\uparrow\downarrow\downarrow\rangle, |\downarrow\uparrow\uparrow\rangle, |\downarrow\uparrow\downarrow\rangle, |\downarrow\downarrow\uparrow\rangle$ and $|\downarrow\downarrow\downarrow\rangle\}$ is an 8×8 matrix.

Exact diagonalization of the Hamiltonian matrix in the basis of eight states yields two quadruplet levels corresponding to total spin $S = 3/2$ and total spin $S = 1/2$. We write the eigenstates of the Hamiltonian in Eq. (1) as $|\alpha, S, S_t^z\rangle$ where α is the index of the eigenstate, S the total spin, and S_t^z the z component of the total spin of the system.

The ground state $S = 3/2$ quadruplet consists of the following four eigenstates with eigenvalue $-\frac{3}{4}J$,

$$\left|1, \frac{3}{2}, \frac{3}{2}\right\rangle = |\uparrow\uparrow\uparrow\rangle, \tag{2}$$

$$\left|2, \frac{3}{2}, -\frac{3}{2}\right\rangle = |\downarrow\downarrow\downarrow\rangle, \tag{3}$$

$$\left|3, \frac{3}{2}, \frac{1}{2}\right\rangle = \frac{1}{\sqrt{3}} [|\downarrow\uparrow\uparrow\rangle + |\uparrow\downarrow\uparrow\rangle + |\uparrow\uparrow\downarrow\rangle], \tag{4}$$

$$\left|4, \frac{3}{2}, -\frac{1}{2}\right\rangle = \frac{1}{\sqrt{3}} [|\uparrow\downarrow\downarrow\rangle + |\downarrow\uparrow\downarrow\rangle + |\downarrow\downarrow\uparrow\rangle]. \tag{5}$$

The four states correspond to the two distinct classes[18] of highly entangled states of a tripartite qubit system. As will be shown below, the mixed $|1\rangle$ and $|2\rangle$ states form the two states of the GHZ class [$|GHZ^\pm\rangle = \frac{1}{\sqrt{2}}(|\uparrow\uparrow\uparrow\rangle \pm |\downarrow\downarrow\downarrow\rangle)$] while $|3\rangle$ and $|4\rangle$ belong to the W class.[13]

The excited quadruplet with total spin $S = 1/2$ and eigenvalue $+\frac{3}{4}J$ are comprised of the following four chiral states:[15,19]

$$\left|5, \frac{1}{2}, \frac{1}{2}\right\rangle = \frac{1}{\sqrt{3}} [|\downarrow\uparrow\uparrow\rangle + e^{\frac{i2\pi}{3}}|\uparrow\downarrow\uparrow\rangle + e^{\frac{i4\pi}{3}}|\uparrow\uparrow\downarrow\rangle], \tag{6}$$

$$\left|6, \frac{1}{2}, \frac{1}{2}\right\rangle = \frac{1}{\sqrt{3}} [|\downarrow\uparrow\uparrow\rangle + e^{-\frac{i2\pi}{3}}|\uparrow\downarrow\uparrow\rangle + e^{-\frac{i4\pi}{3}}|\uparrow\uparrow\downarrow\rangle], \tag{7}$$

$$\left|7, \frac{1}{2}, -\frac{1}{2}\right\rangle = \frac{1}{\sqrt{3}} [|\uparrow\downarrow\downarrow\rangle + e^{\frac{i2\pi}{3}}|\downarrow\uparrow\downarrow\rangle + e^{\frac{i4\pi}{3}}|\downarrow\downarrow\uparrow\rangle], \tag{8}$$

$$\left|8, \frac{1}{2}, -\frac{1}{2}\right\rangle = \frac{1}{\sqrt{3}} [|\uparrow\downarrow\downarrow\rangle + e^{-\frac{i2\pi}{3}}|\downarrow\uparrow\downarrow\rangle + e^{-\frac{i4\pi}{3}}|\downarrow\downarrow\uparrow\rangle]. \tag{9}$$

These chiral states are the eigenstates of the chirality operator $\chi = S_1 \cdot (S_2 \times S_3)$ as described in Ref. 20. The states have the spin ($\uparrow$ and $\downarrow$) currents going in two different ($\circlearrowright$ and $\circlearrowleft$) directions.

For simplicity we shall shift the overall energy scale by $\frac{3}{4}J$ with the energy of the ground state quadruplet as the reference energy. To obtain one of the two GHZ states as a ground state of the system we need to apply a perturbation which will mix the states $|1\rangle$ and $|2\rangle$ while separating them from the remaining two W states, $|3\rangle$ and $|4\rangle$, thus splitting the degenerate eigenspace of the lower quadruplet. As was shown in Ref. 1 this can be accomplished by applying an in-plane radial magnetic field.

We now apply the radial magnetic field B as shown in Fig. 1. The Hamiltonian $H_B = g_e \mu_B \sum_i B_i \cdot S_i$ describing the coupling of the spins to an externally applied in-plane radial magnetic field generated using the two bar magnets placed with similar poles[21] facing each other, as shown in the right panel of Fig. 1, reads

$$H_B = b[\sigma_1^x] + b\left[-\frac{1}{2}\sigma_2^x - \frac{\sqrt{3}}{2}\sigma_2^y\right] + b\left[-\frac{1}{2}\sigma_3^x + \frac{\sqrt{3}}{2}\sigma_3^y\right], \tag{10}$$

where $b = \frac{g_e \mu_B B \hbar}{2}$ is an effective magnetic field with g_e an effective electron g factor in the plane of a quantum dot, μ_B the Bohr magneton, and B the strength of the radial magnetic field at the quantum dot position. The effective magnetic field "b" is simply related to Zeeman energy splitting $2b = \Delta E_z$ for a given external magnetic field "B." And S_i is a vector denoting the spin at quantum dot "i" with Pauli matrices as components along the x and y directions.

The complete Hamiltonian of the three spin system in an external magnetic field is given as

$$H = H_H + H_B. \tag{11}$$

The physical meaning of the radial magnetic field is best described by its action on the spin polarized state

$$H_B|\uparrow\uparrow\uparrow\rangle = \frac{1}{\sqrt{3}} [|\downarrow\uparrow\uparrow\rangle + e^{-\frac{i2\pi}{3}}|\uparrow\downarrow\uparrow\rangle + e^{-\frac{i4\pi}{3}}|\uparrow\uparrow\downarrow\rangle]. \tag{12}$$

Thus the radial in-plane magnetic field simultaneously flips the spins and adds a phase factor in such a way as to generate a chiral state $|6\rangle$ with $S = 1/2, S_t^z = +1/2$ and momentum $k = 2\pi/3$. In a similar way H_B couples state $|6\rangle$ ($S_t^z = +1/2, k = 2\pi/3$) with state $|7\rangle$ ($S_t^z = -1/2, k = -2\pi/3$) and state $|7\rangle$ with spin polarized state $|2\rangle$ with ($S_t^z = -3/2, k = 0$). The

transition from state $|1\rangle$ to state $|2\rangle$ is a third order process in b. The final effective Hamiltonian for the two spin polarized states ($|1\rangle$ and $|2\rangle$) and the two chirality states ($|6\rangle$ and $|7\rangle$) reads,

$$
\left(
\begin{array}{cc|cc}
0 & 0 & b\sqrt{3} & 0 \\
0 & 0 & 0 & b\sqrt{3} \\
\hline
b\sqrt{3} & 0 & \frac{3}{2}J & 2b \\
0 & b\sqrt{3} & 2b & \frac{3}{2}J
\end{array}
\right).
$$

With the radial magnetic field [second term in Eq. (11)] treated as a perturbation, the degenerate perturbation theory[22] leads to an effective 2×2 Hamiltonian matrix (H^{eff}) in the subspace of spin polarized $S = \frac{3}{2}$ states

$$
H^{\mathrm{eff}} = \begin{pmatrix} 0 & \frac{8b^3}{3J^2} \\ \frac{8b^3}{3J^2} & 0 \end{pmatrix}. \tag{13}
$$

The effective Hamiltonian is that of a two level system with tunneling $T = \frac{8b^3}{3J^2}$ proportional to the third power of the external magnetic field "b." After the diagonalization of the matrix in Eq. (13) we obtain as the ground state the GHZ state $|\mathrm{GHZ}^+\rangle = \frac{1}{\sqrt{2}}(|\uparrow\uparrow\uparrow\rangle + |\downarrow\downarrow\downarrow\rangle)$ with energy $-\frac{8b^3}{3J^2}$, separated from the second GHZ state by $2T = \frac{16b^3}{3J^2}$ as also obtained in Ref. 1.

The energy splitting of the two GHZ states can be also written in terms of exchange coupling J and the Zeeman energy as $2T = \frac{2}{3}(\Delta E_z)(\frac{\Delta E_z}{J})^2$. For GaAs $\Delta E_z = 20\ \mu$eV in the field of $B = 1$ Tesla. The exchange coupling measured for coupled lateral GaAs quantum dots is comparable to Zeeman splitting as $J \sim 20\ \mu$eV (Ref. 23). Hence in lateral devices the two GHZ states can be separated on the order of Zeeman energy (i.e., several μeV). The full discussion of physical parameters in gated and self-assembled quantum dots is deferred to the end of Sec. III.

In the next section we discuss how spins of electrons in a quantum dot molecule can be used to realize the GHZ states in solid state quantum dot molecules.

III. QUANTUM DOT MOLECULE

A lateral triple quantum dot molecule (TQDM)[5–7,17,24–26] with one electron per dot is the simplest realization of the three spin system discussed in the previous section. Assuming a single orbital per dot and arbitrary occupation, as shown in Refs. 6 and 7, the quantum dot molecule can be described by an extended Hubbard Hamiltonian,

$$
\mathcal{H}^{\mathrm{QDM}} = \sum_{\substack{i=1 \\ \tau}}^{N} \epsilon_i n_{i\tau} - \sum_{\substack{i,j=1 \\ \tau}}^{N} t_{ij}(c_{i\tau}^{\dagger} c_{j\tau} + \mathrm{H.c.})
$$

$$
+ U \sum_{\substack{i=1 \\ \tau}}^{N} n_{i\tau} n_{i-\tau} + \sum_{i,j=1}^{N} V_{ij} \rho_i \rho_j, \tag{14}
$$

where N is the number of quantum dots ($N = 3$ for TQDM), $c_{i\tau}^{\dagger}$ ($c_{i\tau}$) is the creation (annihilation) operator of an electron with spin $\tau(=\uparrow,\downarrow)$ at the ith quantum dot (QD),

$n_{i\tau}(=c_{i\tau}^{\dagger} c_{i\tau})$ is the spin-dependent electron occupation number, $\rho_i(=\sum_{\tau} n_{i\tau})$ is the total occupation number at site "i," ϵ_i is the on-site energy, t_{ij} is the interdot tunneling matrix element between nearest-neighboring dots "i" and "j," U_i is the intradot and V_{ij} the interdot Coulomb repulsion between the nearest-neighboring dots, and H.c. means the hermitian conjugate.

At half-filling, the Hubbard Hamiltonian reduces to an isotropic Heisenberg Hamiltonian, but with antiferromagnetic exchange coupling,[6,7] $\sim 4t^2/U$, and the ground state (GS) is in the subspace of the total spin $S = \frac{1}{2}$. Thus it is not possible to tune the GS of the system to a maximally spin polarized subspace of $S = \frac{3}{2}$ where the GHZ states reside. However, it was shown[6,17] that the triple quantum dot molecule with four electrons, which corresponds to two holes, has a spin polarized GS. When one of the dots is biased, it contains two spin singlet electrons while the two remaining electrons, localized on the two remaining dots, are coupled ferromagnetically. Biasing the dot further effectively decouples this dot and leaves the remaining two dots with one electron each in a spin singlet state (i.e., coupled antiferromagnetically).

Hence it is, in principle, possible to design a half-filled TQDM combined with auxiliary doubly occupied quantum dots to generate an effective ferromagnetic coupling of spins in the TQDM. If this is accomplished then we can realize the GHZ states in such a quantum dot molecule by applying a radial in-plane magnetic field as explained in the previous section.

In what follows we propose two design structures, namely a six and a four quantum dot molecule as shown on the left and right sides of Fig. 2, respectively. While we studied both, we discuss in detail the six quantum dot molecule because it might be difficult to fabricate a triangular quantum dot structure with a central auxiliary dot in the middle.

We form a six quantum dot molecule (SQDM) by bringing three doubly occupied dots (labeled 4, 5, and 6) close to the central[27] triangle (1, 2, and 3) of singly occupied dots, for a total of nine electrons. The Hamiltonian for SQDM, $\mathcal{H}^{\mathrm{SQD}}$, is given in Eq. (14) for $N = 6$. We consider $t_{ij} = t$ and $V_{ij} = V$
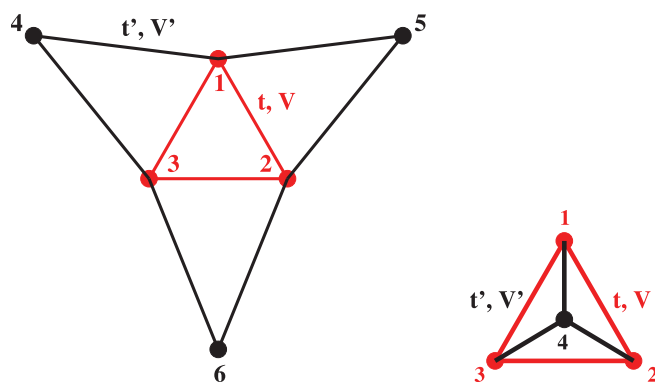

FIG. 2. (Color online) Left: Schematic of a six dot molecule with dots labeled 1, 2, and 3 forming the central triple quantum dot molecule and dots 4, 5, and 6 are the auxiliary dots. Right: A four dot molecule structure with dot 4 being an additional dot introduced to the triple quantum dot molecule (1,2,3).

for the central triangle $\{i,j\} = \{1,2,3\}$ and $t_{ij} = t'$ and $V_{ij} = V'$ for all other dots as shown in the left panel of Fig. 2.

We create all 220 $N_e = 9$ electron configurations $\prod_{i,\sigma} c^+_{i,\sigma} |0\rangle$, construct the Hamiltonian matrix, and diagonalize it numerically to obtain the energy spectrum and eigenvectors. In the absence of the magnetic field the z component of the total spin is a good quantum number giving the Hamiltonian matrix in a block diagonal form. The Hilbert space dimensions of the blocks in the subspace of the z component of total spin $S^z_t = \pm\frac{1}{2}$ and $S^z_t = \pm\frac{3}{2}$ are 90 and 20, respectively. Each block is numerically diagonalized so as to obtain the GS of the system as a function of the Hubbard parameters.

In our calculations we assume $\epsilon_1 = \epsilon_2 = \epsilon_3 = 0$ [i.e., the dots (1,2,3) are on resonance]. The energy $\epsilon_4 = \epsilon_5 = \epsilon_6 = \epsilon$ of auxiliary dots is varied by applied gate voltage. We consider the regime $U \gg t, V$ with a constant value of $U = 2.0$, $V = 0.1$ as considered earlier.[28] We vary interdot Coulomb repulsion and tunneling between the central and auxiliary dots as $0 < V' < V$ and $0 < t' < t$. All the parameters are in the unit of the effective Rydberg defined by $Ry = m^* e^4 / 2\epsilon_0^2 \hbar^2$ where m^* is the electron effective mass, e the electron charge, and ϵ_0 the dielectric constant of a material. For example, in the case of GaAs the effective Rydberg is estimated to be about 6 meV.

The GS of the system is a linear superposition of the basis used to construct the Hamiltonian matrix in that given subspace. For certain parameters the GS contains the spin polarized configuration with spins localized on the three dots. This is illustrated in Fig. 3 which shows the dominant configuration, with probability 0.9289 for the GS in the subspace of total spin $S = \frac{3}{2}$ and the z component of total spin $S^z_t = \frac{3}{2}$ obtained for parameters $\epsilon = -0.05$, $U = 2.0$, $V = 0.1$, $t = 0.05$, $V' = 0.094$, and $t' = 0.05$. It is clearly seen that the three electron spins are localized on the triangle of dots (1,2,3) forming the ferromagnetically coupled three spin system and the auxiliary dots (4,5,6) are doubly occupied, driving the GS of the quantum dot molecule to be in the maximally spin polarized subspace.

We define a state corresponding to the dominant charge configuration in the subspace of the z component of total spin $S^z_t = \frac{3}{2}$ as,

$$|US\rangle = |(\uparrow_1\uparrow_2\uparrow_3)(\uparrow_4\downarrow_4\uparrow_5\downarrow_5\uparrow_6\downarrow_6)\rangle, \quad (15)$$
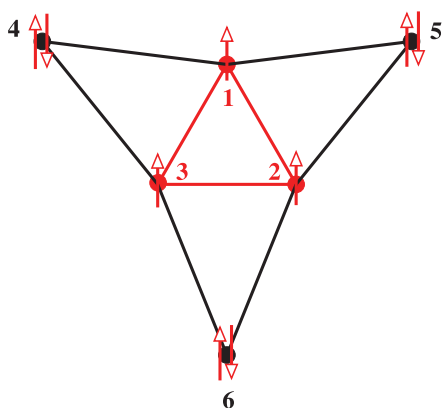

FIG. 3. (Color online) Dominant charge configuration in the subspace of total spin $S = \frac{3}{2}$ and z component of total spin $S^z_t = \frac{3}{2}$ for a six dot molecule with nine electrons.

with a similar definition for the dominant charge configuration in the subspace of the z component of total spin $S^z_t = -\frac{3}{2}$ as,

$$|DS\rangle = |(\downarrow_1\downarrow_2\downarrow_3)(\uparrow_4\downarrow_4\uparrow_5\downarrow_5\uparrow_6\downarrow_6)\rangle. \quad (16)$$

We now determine the set of parameters for which the SQDM describes the three spin system well, that is, we calculate the overlap probability at zero magnetic field ($B = 0$),

$$P_{B=0} = |\langle GS|US\rangle|^2, \quad (17)$$

of the numerically obtained GS with state $|US\rangle$ as a function of parameters. The nonzero overlap probability as a function of parameters t, t', V', and ϵ for fixed U, V determines the phase diagram region in parameter space where the three electrons are localized on the three dots and interact ferromagnetically. The result of the numerical calculation for $U = 2.0$ and $V = 0.1$ is shown in Fig. 4.

We observe that for a fixed value of t, if we vary ϵ the region of the GS in maximally spin polarized subspace gets reduced, but the maximum value of the overlap probability increases marginally. This happens because as we lower the on-site energies of the auxiliary dots, the three central dots become isolated from the auxiliary system and behave like half-filled TQDM. And so a higher value of t' is required to have the GS in maximally spin polarized subspace. Hence the region belonging to the total spin $S = \frac{3}{2}$ decreases.

It is also found that for a fixed ϵ, varying t decreases the maximum value of the overlap probability, but the region of GS
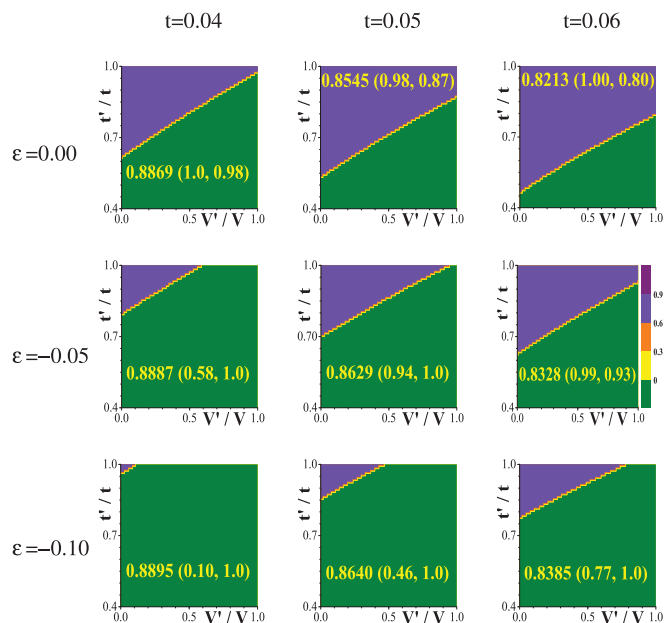

FIG. 4. (Color online) Phase diagram of GS overlap probability with a state of dominant charge configuration in the subspace of $S = \frac{3}{2}$ for a six quantum dot molecule is shown as a function of t'/t and V'/V. The individual view graphs are for different values of hopping element t and the on-site energy ϵ at dots (4,5,6). The lower area in each graph (green in color) denotes the GS is in the subspace of total spin $S = \frac{1}{2}$ and its overlap is zero. The number in each graph corresponds to the maximum value of the overlap probability at the point given in the bracket.

in maximally spin polarized subspace increases. It is because of increasing the tunneling, t, delocalizes the electrons in the central TQD molecule which decreases the contribution of the spin polarized configuration, Eq. (15). But in this scenario even a small value of tunneling t' between the central and auxiliary dots can drive the GS in the maximally spin polarized subspace and so the area comprising of the GS in total spin $S = \frac{3}{2}$ increases.

It is also observed that the maximum value of the overlap probability lies along the border line dividing the regions where the GS is in the subspace of total spin $S = \frac{1}{2}$ (zero probability) and that of total spin $S = \frac{3}{2}$ (finite probability).

Choosing an appropriate set of parameters can maximize the overlap probability and prepare the GS of the system with the spin polarized charge configuration given in Eq. (15). We thus define a GHZ state for the SQDM system as,

$$|GHZ^{\pm}\rangle = \frac{1}{\sqrt{2}}[|US\rangle \pm |DS\rangle]. \quad (18)$$

To form one of the states given in Eq. (18) as a GS of the SQDM we apply a radial in-plane magnetic field as shown in Fig. 5. The Hamiltonian describing this interaction of the electron spins with external magnetic field is $\mathcal{H}^B = g_e \mu_B \sum_{i=1}^{6} \mathbf{B}_i \cdot \mathbf{S}_i$ and is given as

$$\mathcal{H}^B = b[\sigma_1^x] + b\left[-\frac{1}{2}\sigma_2^x - \frac{\sqrt{3}}{2}\sigma_2^y\right] + b\left[-\frac{1}{2}\sigma_3^x + \frac{\sqrt{3}}{2}\sigma_3^y\right]$$
$$+ b\left[\frac{1}{2}\sigma_4^x + \frac{\sqrt{3}}{2}\sigma_4^y\right] + b\left[\frac{1}{2}\sigma_5^x - \frac{\sqrt{3}}{2}\sigma_5^y\right] + b[-\sigma_6^x]. \quad (19)$$

The spin operators (σ^x, σ^y) are written in a second quantized form as

$$\sigma_j^x = \frac{1}{2}[c_{j\uparrow}^{\dagger} c_{j\downarrow} + c_{j\downarrow}^{\dagger} c_{j\uparrow}], \quad (20)$$
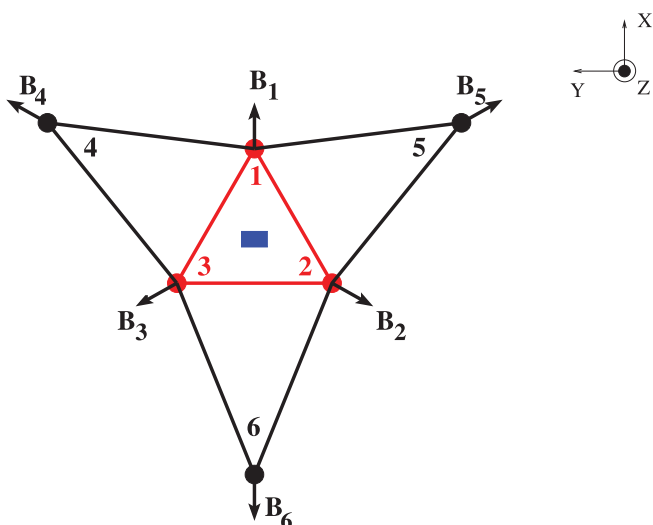

FIG. 5. (Color online) Schematic depicting top bar magnets (rectangular box shown in blue) with like poles facing each other are placed at the center of the system which generates a radial in-plane magnetic field.

and

$$\sigma_j^y = \frac{i}{2}[c_{j\downarrow}^{\dagger} c_{j\uparrow} - c_{j\uparrow}^{\dagger} c_{j\downarrow}]. \quad (21)$$

We write the complete Hamiltonian for SQDM and an applied external magnetic field as,

$$\mathcal{H} = \mathcal{H}^{QDM} + \mathcal{H}^B, \quad (22)$$

and the Hamiltonian matrix is constructed using the same basis as used to create $\mathcal{H}^{SQD}$. But since the magnetic field does not preserve the spin rotational symmetry the Hamiltonian matrix in Eq. (22) is not in a block diagonal form. The dimension of the full Hilbert space is 220. We diagonalize the Hamiltonian matrix for three different values of ϵ and tunneling matrix element, t. These are chosen such that, in the absence of an external magnetic field, the area covered by the subspace of total spin $S = \frac{3}{2}$ in each view graph of Fig. 4 is (i) minimum [$\epsilon = -0.10, t = 0.04$], (ii) intermediate [$\epsilon = -0.05, t = 0.05$], and (iii) maximum [$\epsilon = 0.00, t = 0.06$]. And for each value of ϵ and t, we diagonalize the Hamiltonian matrix for the parameters $(\frac{V'}{V}, \frac{t'}{t})$ where the overlap probability, Eq. (17), is maximum.

At these points the low energy spectrum of the extended Hubbard Hamiltonian resembles the energy spectrum of an isotropic Heisenberg Hamiltonian with four-fold degenerate ground and excited state as discussed in the previous section. For zero magnetic field the energy separation between these two degenerate states is $\frac{3J}{2}$. We use this to find the values of ferromagnetic exchange, J, in our Hubbard model for parameters (t, t', V, V', ϵ) mentioned above with fixed U, V and we use it as our energy scale.

For each set of parameters, the exact diagonalization of Eq. (22) yields the two GHZ states as the ground and first excited states of our system. In Sec. II for the Heisenberg system, we have seen that the energy separation between the two GHZ states for a finite magnetic field is $\approx \frac{16b^3}{3J^2}$ where b is the effective strength of the magnetic field. Apart from the Heisenberg model, we calculate the energy splitting between the two GHZ states for our Hubbard model as a function of $\frac{2b}{J}$ for three different values of ϵ, t, and corresponding J. The result is shown in Fig. 6. We observe that for smaller values of $\frac{b}{J}$, the Heisenberg and Hubbard models behave similarly but for larger values the agreement is worse. But it is also seen (inset of Fig. 6) that as we keep on decreasing ϵ and t the energy gap obtained from the Hubbard model starts approaching the Heisenberg model. This is expected since the value of the maximum overlap probability is smallest for ($\epsilon = 0.00, t = 0.06$) and largest for ($\epsilon = -0.10, t = 0.04$).

Using the same set of Hubbard parameters, we also evaluate the maximum overlap probability of the GS with one of the GHZ state for the SQDM as given in Eq. (18) for a finite magnetic field and denote it as

$$P_{B \neq 0} = |\langle GS|GHZ^+\rangle|^2. \quad (23)$$

The results are shown in Fig. 7 as a function of ϵ, t, and J. We find that as the strength of the effective magnetic field, b, approaches the value of J the GS of the Hubbard model deviates more and more from the GHZ state for SQDM which results in the decrease of the overlap probability.
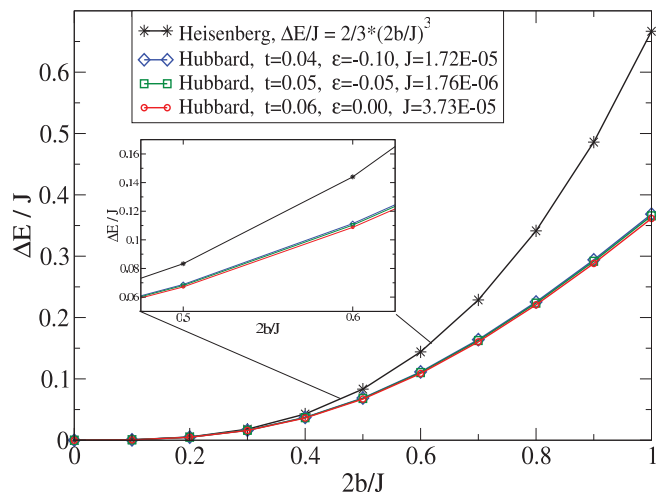
FIG. 6. (Color online) Energy splitting between the two GHZ states is shown as a function of $\frac{2b}{J}$ for three different values of ϵ, t, and J. The stars represent the results as obtained for the three spin system, Heisenberg model.

We now turn to the discussion of the physical parameters and structures needed for the realization of the GHZ generator. Typical parameters leading to an effective ferromagnetic coupling of three spins localized on a triangle, shown in Fig. 4, involve $U = 2$, $V = 0.1$, $t = 0.05$, $t' \leqslant t$, and $V' \leqslant V$ and a bias ϵ of the order of tunneling, t. The values currently available for lateral gated quantum dots on GaAs are in the required parameter ranges of $U \sim 2$, $V \sim 0.1$, and $t \sim 0.05$ meV. By building quantum dot networks using individually gated self-assembled quantum dots on nanotemplates[29] one can envisage reaching values of parameters for self-assembled quantum dots $U \sim 20$, $V \sim 10$, $t \sim 10$ meV which should lead to the exchange coupling reaching $J \sim 40$ meV, exceeding room temperature.

Finally, we discuss the lifetime of a maximally entangled GHZ state. Since in the proposed scheme the GHZ state is the GS, it is expected to only suffer decoherence and no population decay. If the quantum dot molecule is realized in GaAs, nuclear spins are expected to be the major source of decoherence. Since the problem of decoherence of the GHZ state is common with a single electron spin, recently developed coherent control of nuclear spins[30] might be expected to be
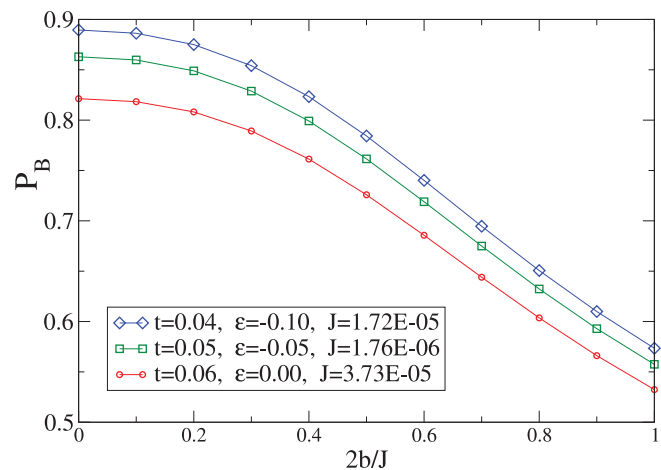

FIG. 7. (Color online) Maximum overlap probability of the GS with GHZ^+ is shown as a function of $\frac{2b}{J}$ for three different values of ϵ, t, and J.

applicable in extending the coherence of the GHZ state. This problem will be investigated in the future.

IV. SUMMARY AND CONCLUSION

In summary, we designed and analyzed theoretically a lateral quantum dot molecule combined with a micromagnet generating a maximally entangled three particle GHZ GS. The quantum dot molecule consists of three quantum dots with one electron spin each forming a central equilateral triangle. The antiferromagnetic spin-spin interaction is changed to the ferromagnetic interaction by additional doubly occupied quantum dots, one dot near each side of a triangle. Exact diagonalization studies of the Hubbard model of the molecule determine the phase diagram in parameter space and a set of parameters is established for which the GS of the molecule in a radial magnetic field is well approximated by a GHZ state.

*anand.sharma@nrc-cnrc.gc.ca; Present address: Department of Physics, 82 University Place, University of Vermont, Burlington, VT.

†pawel.hawrylak@nrc-cnrc.gc.ca

[1]B. Röthlisberger, J. Lehmann, D. S. Saraga, P. Traber, and D. Loss, Phys. Rev. Lett. **100**, 100502 (2008).

[2]D. M. Greenberger, M. A. Horne, and A. Zeilinger, in *Bell's Theorem, Quantum Theory, and Conceptions of the Universe*, edited by M. Kafatos (Kluwer Academic, Dordrecht, 1989); D. M. Greenberger, M. A. Horne, A. Shimony, and A. Zeilinger, Am. J. Phys. **58**, 1131 (1990); N. D. Mermin, Phys. Today **43**, 9 (1990).

[3]D. Bohm, *Quantum Theory* (Prentice Hall, New York, 1951).

[4]M. A. Nielsen and I. L. Chuang, *Quantum Computation and Quantum Information* (Cambridge University Press, New York, 2000).

[5]L. Gaudreau, S. A. Studenikin, A. S. Sachrajda, P. Zawadzki, A. Kam, J. Lapointe, M. Korkusinski, and P. Hawrylak, Phys. Rev. Lett. **97**, 036807 (2006).

[6]M. Korkusinski, I. P. Gimenez, P. Hawrylak, L. Gaudreau, S. A. Studenikin, and A. S. Sachrajda, Phys. Rev. B **75**, 115301 (2007).

[7]I. Puerto Gimenez, M. Korkusinski, and P. Hawrylak, Phys. Rev. B **76**, 075336 (2007).

[8]L. Quiroga and N. F. Johnson, Phys. Rev. Lett. **83**, 2270 (1999); J. A. Reina and N. F. Johnson, Phys. Rev. A **63**, 012303 (2000).

[9]S.-B. Zheng, Phys. Rev. Lett. **87**, 230404 (2001).

[10]M. D. Kim and S. Y. Cho, Phys. Rev. B **77**, 100508(R) (2008).

[11] D. Bouwmeester, J.-W. Pan, M. Daniell, H. Weinfurter, and A. Zeilinger, Phys. Rev. Lett. **82**, 1345 (1999); J.-W. Pan, D. Bouwmeester, M. Daniell, H. Weinfurter, and A. Zeilinger, Nature (London) **403**, 515 (2000).

[12] A. Rauschenbeutel, G. Nogues, S. Osnaghi, P. Bertet, M. Brune, J.-M. Raimond, and S. Haroche, Science **288**, 2024 (2000).

[13] M. Neeley, R. C. Bialczak, M. Lenander, E. Lucero, M. Mariantoni, A. D. O'Connell, D. Sank, H. Wang, M. Weides, J. Wenner, Y. Yin, T. Yamamoto, A. N. Cleland, and J. M. Martinis, Nature (London) **467**, 570 (2010).

[14] L. DiCarlo, M. D. Reed, L. Sun, B. R. Johnson, J. M. Chow, J. M. Gambetta, L. Frunzio, S. M. Girvin, M. H. Devoret, and R. J. Schoelkopf, Nature (London) **467**, 574 (2010).

[15] P. Hawrylak, Phys. Rev. Lett. **71**, 3347 (1993).

[16] L. Jacak, P. Hawrylak, and A. Wojs, *Quantum Dots* (Springer, Berlin, 1998); A. S. Sachrajda, P. Hawrylak, and M. Ciorga, in *Electronic Transport in Quantum Dots*, edited by J. P. Bird (Kluwer Academic, Boston, 2003).

[17] Y.-P. Shim and P. Hawrylak, Phys. Rev. B **78**, 165317 (2008).

[18] W. Dür, G. Vidal, and J. I. Cirac, Phys. Rev. A **62**, 062314 (2000); A. Acín, D. Bruß, M. Lewenstein, and A. Sanpera, Phys. Rev. Lett. **87**, 040401 (2001).

[19] V. Subrahmanyam, Phys. Rev. B **50**, 6468 (1994).

[20] C.-Y. Hsieh and P. Hawrylak, Phys. Rev. B **82**, 205311 (2010).

[21] In Fig. 1 we assume a field direction pointing radially outward by considering two north poles facing each other. But a field direction pointing inward by making the two south poles face each other can also be considered.

[22] P. O. Löwdin, J. Chem. Phys. **19**, 1396 (1951).

[23] A. C. Johnson, J. R. Petta, J. M. Taylor, A. Yacoby, M. B. Lukin, C. M. Marcus, M. P. Hanson, and A. C. Gossard, Nature (London) **435**, 925 (2005).

[24] D. Schröer, A. D. Greentree, L. Gaudreau, K. Eberl, L. C. L. Hollenberg, J. P. Kotthaus, and S. Ludwig, Phys. Rev. B **76**, 075306 (2007).

[25] P. Hawrylak and M. Korkusinski, Solid State Commun. **136**, 508 (2005).

[26] F. Delgado, Y.-P. Shim, M. Korkusinski, and P. Hawrylak, Phys. Rev. B **76**, 115332 (2007).

[27] In plane geometry it would be termed as Morley's triangle. The interested reader can refer to C. Kimberling, Congr. Numer. **129**, 1 (1998).

[28] Y.-P. Shim, A. Sharma, C.-Y. Hsieh, and P. Hawrylak, Solid State Commun. **150**, 2065 (2010).

[29] D. Dalacu, M. E. Reimer, S. Fréderick, D. Kim, J. Lapointe, P. J. Poole, G. C. Aers, R. L. Williams, W. Ross McKinnon, M. Korkusinski, and P. Hawrylak, Laser & Photonics Reviews **4**, 283 (2010).

[30] S. Foletti, H. Bluhm, D. Mahalu, V. Umansky, and A. Yacoby, Nat. Phys. **5**, 903 (2009); H. Bluhm, S. Foletti, D. Mahalu, V. Umansky, and A. Yacoby, Phys. Rev. Lett. **105**, 216803 (2010).